Exit from Arsenite-Induced Mitotic Arrest Is p53 Dependent

Samuel C. McNeely,[1] Xiaoqiang Xu,[1] B. Frazier Taylor,[1] Wolfgang Zacharias,[1,2,3,4] Michael J. McCabe Jr.,[5] and J. Christopher States[1,3,4]

[1]Department of Pharmacology and Toxicology, [2]Department of Medicine, [3]James Graham Brown Cancer Center, and [4]Center for Genetics and Molecular Medicine, University of Louisville, Louisville, Kentucky, USA; [5]Department of Environmental Medicine, University of Rochester, Rochester, New York, USA

BACKGROUND: Arsenic is both a human carcinogen and a chemotherapeutic agent, but the mechanism of neither arsenic-induced carcinogenesis nor tumor selective cytotoxicity is clear. Using a model cell line in which p53 expression is regulated exogenously in a tetracycline-off system (TR9-7 cells), our laboratory has shown that arsenite disrupts mitosis and that p53-deficient cells [p53[(–)]], in contrast to p53-expressing cells [p53[(+)]], display greater sensitivity to arsenite-induced mitotic arrest and apoptosis.

OBJECTIVE: Our goal was to examine the role p53 plays in protecting cells from arsenite-induced mitotic arrest.

METHODS: p53[(+)] and p53[(–)] cells were synchronized in G_2 phase using Hoechst 33342 and released from synchrony in the presence or absence of 5 μM sodium arsenite.

RESULTS: Mitotic index analysis demonstrated that arsenite treatment delayed exit from G_2 in p53[(+)] and p53[(–)] cells. Arsenite-treated p53[(+)] cells exited mitosis normally, whereas p53[(–)] cells exited mitosis with delayed kinetics. Microarray analysis performed on mRNAs of cells exposed to arsenite for 0 and 3 hr after release from G_2 phase synchrony showed that arsenite induced inhibitor of DNA binding-1 (ID1) differentially in p53[(+)]and p53[(–)] cells. Immunoblotting confirmed that ID1 induction was more extensive and sustained in p53[(+)] cells.

CONCLUSIONS: p53 promotes mitotic exit and leads to more extensive ID1 induction by arsenite. ID1 is a dominant negative inhibitor of transcription that represses cell cycle regulatory genes and is elevated in many tumors. ID1 may play a role in the survival of arsenite-treated p53[(+)] cells and contribute to arsenic carcinogenicity.

KEYWORDS: apoptosis, arsenite, ID1, microarray, mitotic arrest, p53. *Environ Health Perspect* 114:1401–1406 (2006). doi:10.1289/ehp.8969 available via *http://dx.doi.org/* [Online 23 June 2006]

Arsenic is both a human carcinogen causing cancer in multiple tissues [National Research Council (NRC) 1999, 2001] and a chemotherapeutic agent used in the treatment of acute promyelocytic leukemia (Cohen et al. 2001). Arsenic trioxide shows promise for chemotherapy in treatment of solid tumors and inhibits tumor growth in an orthotopic prostate cancer model (Maeda et al. 2001). However, the mechanism by which arsenic selectively induces cell death in tumor cells is not understood.

Clinically achievable concentrations of arsenite induce cell death in a variety of cancer cell lines and virally immortalized cell lines that lack normal cell cycle control. Arsenic trioxide (As_2O_3) induces apoptosis in several prostate and ovarian cancer cell lines (Du and Ho 2001; Uslu et al. 2000). Arsenite induces mitotic arrest and apoptosis in SV40-transformed human fibroblasts (States et al. 2002), spontaneously immortalized p53-deficient Li-Fraumeni human fibroblasts (Taylor et al. 2006), and in HeLa S3 and KB cells (Huang and Lee 1998). In contrast, these moderate concentrations of arsenite slow the growth of diploid human fibroblasts but do not induce cell death (States et al. 2002; Yih et al. 1997). However, arsenite disrupts normal mitotic progression and induces aneuploidy in human diploid fibroblasts (Yih et al. 1997) and peripheral blood lymphocytes (Vega et al. 1995).

A common feature of the cell lines in which arsenite induces apoptosis is a p53-deficient phenotype, either by mutation or viral oncogene inactivation of p53. p53 regulates cell cycle progression and apoptosis in response to genetic damage. The molecular mechanisms by which p53 arrests cell cycle progression in G_1 and G_2 phases in response to DNA damage are reasonably well understood (Jin and Levine 2001). p53 is activated in response to mitotic disruption by arsenic (Yih and Lee 2000). However, the signals for p53 activation and the role that p53 plays in the cellular response to mitotic disruption are not clear.

In asynchronous TR9-7 cells (human fibroblasts with tetracycline-regulated p53 expression), arsenite treatment induces a p53-independent accumulation of cells with G_2/M phase DNA content (Taylor et al. 2006). However, accumulation of mitotic cells occurs in p53-deficient [p53[(–)]] but not in p53-expressing [p53[(+)]] TR9-7 cells. Furthermore, the mitotically arrested p53[(–)] cells undergo apoptosis, whereas most p53[(+)] cells exit G_2/M phase and arrest in G_1 phase. Therefore, we hypothesized that p53 did not prevent delayed G_2 transit but did protect against apoptosis subsequent to the arsenite-induced mitotic arrest.

To investigate the role of p53 in the arsenite-induced disruption of G_2/M phase progression, we examined the response of p53[(+)] and p53[(–)] TR9-7 cells to arsenite treatment after release from G_2 phase synchrony. We show that in synchronized TR9-7 cells arsenite delayed entry into mitosis independently of p53 expression but that the exit from mitosis in arsenite-treated cells was p53 dependent. Furthermore, we show that the apoptotic process occurred while the cells attempted cytokinesis. We hypothesized the difference in exit kinetics and resistance to apoptosis between p53[(+)] and p53[(–)] cells was due to p53-mediated alterations of gene expression profiles. Microarray analysis of G_2 phase–synchronized p53[(+)] and p53[(–)] cells treated with arsenite for 3 hr revealed p53-dependent induction of inhibitor of DNA binding-1 (ID1). Negative transcriptional regulation of cyclin-dependent kinase inhibitors by ID1 may have implications for cell cycle progression in p53[(+)] cells surviving arsenite-induced mitotic perturbation and may play a role in arsenic-induced carcinogenesis.

Materials and Methods

Cell culture and synchronization. TR9-7 cells were the gift of M.A. Tainsky (Wayne State University, Detroit, MI). Cells were cultured at 37ºC at 5% CO_2 in a humidified incubator in alpha modification of minimal essential media (GIBCO/BRL, Gaithersburg, MD) supplemented with 10% fetal bovine serum (HyClone, Logan, UT), 10 mM HEPES (pH 7.0), 200 μg/mL geneticin (Invitrogen Corp., Carlsbad, CA), 40 μg/mL hygromycin B (Sigma Chemical Co., St. Louis, MO), 100 U/mL penicillin, and 10 U/mL streptomycin.

Cells were synchronized in G_2 phase of the cell cycle according to adaptation of published procedures (Kuhholzer and Prather 2001; Tobey et al. 1990). Briefly, we plated cells in the presence of 15 ng/mL tetracycline (Fisher Scientific, Pittsburgh, PA) to allow moderate

p53 expression. We replaced media with media containing 5 μg/mL aphidicolin (Sigma) and incubated the cells for 24 hr. We then washed the cells with phosphate-buffered saline (PBS) and incubated them in media containing 0.1 μg/mL Hoechst 33342 (Sigma) for 12 hr. After 6 hr of incubation with Hoechst 33342, p53 expression was suppressed in half the cultures by direct addition of tetracycline (1 mg/mL) to the media to a final concentration of 1,500 ng/mL. Cells were released from G_2 phase by washing with PBS and refeeding with fresh drug-free media.

Arsenic compounds. We prepared fresh working aqueous solutions of sodium arsenite ($NaAsO_2$) (Sigma) on the day of treatment and filter sterilized prior to use.

Flow cytometry. For DNA content analysis, cells were harvested by trypsinization and fixed in 1 mL ice-cold 70% ethanol. Following fixation overnight at 4°C, we centrifuged the samples at $1,500 \times g$ and resuspended the resulting cell pellets in PBS containing propidium iodide and 100 U/mL RNase A (Sigma) for 30 min at room temperature. We analyzed propidium iodide–stained samples on a FACSCalibur (Becton Dickinson and Co., San Jose, CA) using doublet discrimination. Propidium iodide fluorescence was collected on channel two (FL2) (585/42 nm) using linear amplification. A minimum of 20,000 events/sample was analyzed. Data were collected using CellQuest software (Becton Dickinson) and analyzed for cell cycle distribution using Modfit software (Verity Software House, Inc., Topsham, ME).

Mitotic indices. Cells were harvested for mitotic index analysis by trypsinization. Media, wash, and cells were collected together and centrifuged. We resuspended cell pellets in 150 μL serum free media and added 2.5 mL of 0.4% KCl. We incubated the suspension for 10 min at 37°C, then added methanol:acetic acid fixative solution (3:1, vol/vol) to 2% (vol/vol) and collected cells by centrifugation. Cells were resuspended in 2.5 mL fixative solution and fixed at room temperature for 20 min. Samples were centrifuged; cell pellets were resuspended in 0.5 mL fixative and chilled on ice for 1 hr. Aliquots of the suspensions were dropped onto glass slides, air dried, and stained with Wright Giemsa solution (Fisher). We examined slides under a microscope and counted a minimum of 200 cells to determine mitotic index.

Western blot analyses. Media from culture dishes were removed and collected along with one PBS wash. Floating cells were pelleted via centrifugation, washed once with PBS, and lysed with lysis buffer [10 mM Tris–HCl (pH 7.4), 1 mM Na_2–EDTA, 0.1% SDS, 180 μg/mL phenylmethylsulfonyl fluoride]. Adherent cells were lysed directly in the plates. Lysates from floating and adherent fractions

were then combined. Protein concentration in the lysates was determined by Bradford assay (BioRad Laboratories, Inc., Hercules, CA). Proteins were resolved by SDS–PAGE in 12% polyacrylamide gels and transferred to supported nitrocellulose membranes by electroblotting. p53, β-actin, and ID1 were detected by probing membranes with antibodies for p53 (LabVision, Fremont, CA), β-actin (Sigma), or ID1 (Santa Cruz Biotechnologies, Santa Cruz, CA), respectively. Blots were incubated with secondary anti-mouse or anti-rabbit antibody conjugated to horse radish peroxidase (Zymed Laboratories, San Francisco, CA) and visualized with enhanced chemiluminescence (Amersham Biosciences Inc., Piscataway, NJ).

Statistical analyses. Comparison of mitotic indices of arsenite-treated p53[(+)] and p53[(–)] cells was performed by Student t-test using SlideWrite software (version 6.10; Advanced Graphics Software, Encinitas, CA) and confirmed by analysis of variance (ANOVA).

Microarray analyses. We harvested cells via trypsinization and prepared poly(A)[+]

mRNAs using Micro-FastTrack (Invitrogen Corp.). SuperScript II (Invitrogen Corp.) was used with an oligo(dT) primer linked to the T7 RNA polymerase-binding site sequence to synthesize cDNAs. cDNAs were extracted with phenol:chloroform:isoamyl alcohol (25:24:1), precipitated with NH_4OAc and ethanol, and resuspended in RNase-free water. We synthesized biotin-labeled cRNA with an ENZO RNA transcript labeling kit (Enzo Life Sciences, Farmingdale, NY), using 0.7 μg cDNA per reaction. cRNAs were purified with RNeasy purification columns (Qiagen, Valencia, CA). cRNA, 15 μg per sample, was heated at 80°C for 33 min in fragmentation buffer (Affymetrix, Inc., Santa Clara, CA). Fragmented cRNAs were hybridized to U95Av2 GeneChips (Affymetrix) for 16 hr at 45°C. GeneChips were stained with streptavidin phycoerythrin stain solution (Affymetrix). Signal was amplified with goat anti-streptavidin antibody and biotinylated goat IgG (Affymetrix). We scanned stained GeneChips on an Agilent GeneArray Scanner (Agilent Technologies, Palo Alto, CA) and performed four biological replicates.
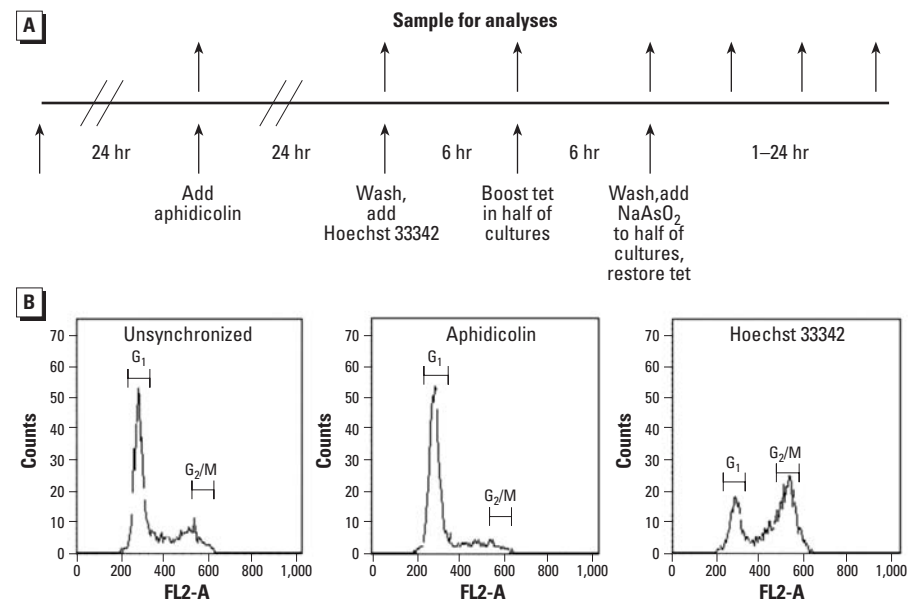
Figure 1. Synchronization of TR9-7 cells expressing or not expressing p53 in G_2 phase. Abbreviations: FL2-A, propidium iodide fluorescence on channel two; Tet, tetracycline. (*A*) Experimental design. (*B*) Cell cycle distribution of synchronized cells. Samples were harvested after treatments indicated and analyzed by flow cytometry. Positions of cells with G_1 and G_2/M phase DNA content are indicated.

Figure 2. p53 and ID1 expression in cells after G_2 phase synchronization. Cells were synchronized, treated with 5 μM $NaAsO_2$, and samples were taken at the indicated times. Levels of p53 and ID1 proteins were assessed by Western blot analysis with β-actin as a loading control. 0 hr = release from Hoechst 33342. A representative example is shown.

We performed ANOVA of the signal data with Bioconductor/R software using MAS (Microarray Suite software) background correction, quantiles normalization, MAS PM (perfect match) correction, MAS summary, and statistical significance defined as $p < 0.05$. Data were filtered on p53 status and arsenite exposure. Analysis was conducted with and without application of the Benjamini and Hochberg false discovery rate correction. Venn analysis was conducted on gene lists using GeneSpring software (Agilent Technologies).

Results

To determine the role that p53 plays in preventing arsenite-induced accumulation of mitotic cells and in preventing arsenite-induced apoptosis, TR9-7 cells were synchronized in G_2 using Hoechst 33342. Hoechst 33342 is a topoisomerase inhibitor that interferes with chromatin condensation, resulting in G_2 phase arrest (Kuhholzer and Prather 2001). The effects of arsenite treatment on the progression from G_2 phase and through mitosis of synchronized p53$^{(+)}$) and p53$^{(-)}$ cells

Figure 3. Arsenite treatment delays mitotic entry, and p53 deficiency delays mitotic exit in arsenite-treated cells. Abbreviations: As$^{(+)}$, + 5 µg sodium arsenite; As$^{(-)}$, 0 µg sodium arsenite. (*A*) Mitotic indices of TR9-7 cells released from G_2 phase synchronization. Mean ± SD from four independent experiments performed with triplicate cultures are plotted. Not all time points assayed in every experiment. (*B*) Arsenite-treated TR9-7 cells in late anaphase/early telophase undergoing apoptosis. Cells were released from G_2 phase by feeding with fresh media containing 5 µM NaAsO$_2$ and monitored by phase microscopy. Photographs in panels 1–8 were taken in order over a 30-min period. Bar, 5 µm.
*Significant difference between arsenite-exposed p53$^{(+)}$ and p53$^{(-)}$ cells.

were evaluated after release from Hoechst 33342-induced G_2 phase synchronization.

TR9-7 cells are a spontaneously immortalized human fibroblast cell line, derived from a Li-Fraumeni patient, and subsequently stably transfected with a tetracycline-regulated p53 expression vector (Yin et al. 1992). p53 expression in TR9-7 cells is inversely proportional to the tetracycline concentration in the media (tet-off). Absence of tetracycline strongly induces p53 and causes TR9-7 cells to arrest in G_1 and G_2 phases (Agarwal et al. 1995). Tetracycline at a concentration of 15 ng/mL induces p53 to a modest level that allows the cells to grow at a rate comparable to p53$^{(-)}$ TR9-7 cells (Taylor et al. 2006).
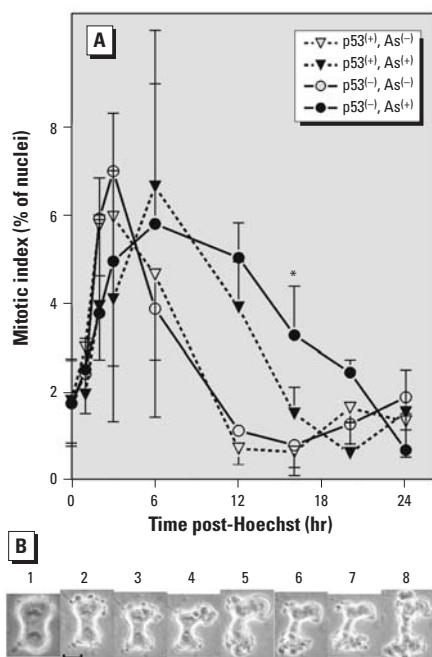
Synchronization of TR9-7 cells in G_2 phase using Hoechst 33342. Synchronization of TR9-7 cells in G_2 phase required plating cells with moderate p53 expression. Cells with high levels of p53 tended to arrest in G_1 or G_2 phase and not re-enter the cell cycle. In addition, induction of p53 by lowering the tetracycline concentration proved difficult to time reproducibly. We obtained reproducible changes in p53 expression by repressing p53 by addition of tetracycline (data not shown). The experimental design we developed is presented in Figure 1. Cells were synchronized in G_1 phase by addition of aphidicolin after allowing freshly plated cells to attach and to acclimate for 24 hr. Cells were released from G_1 phase synchrony after 24-hr aphidicolin exposure by washing the cells and applying fresh media containing Hoechst 33342, which induced G_2 phase synchrony. After 6 hr of incubation in Hoechst 33342 media, p53 transcription was suppressed in half the cultures by addition of tetracycline to 1,500 ng/mL. Cells were incubated for an additional 6 hr. At this point, media were changed again and half of each tetracycline group received media containing 0 or 5 µM NaAsO$_2$ with tetracycline appropriate to maintain p53 expression levels. Samples were taken at each change of media and at

several time points post-Hoechst 33342 incubation. Samples were analyzed with flow cytometry to determine cell cycle distribution (Figure 1B), by Western blot to determine p53 and ID1 expression (Figure 2), and for mitotic spread analysis to determine mitotic index (Figure 3A). We performed microarray analysis to determine changes in gene expression (Tables 1–3).

Cell cycle distribution of synchronized cells. Using the procedure depicted in Figure 1A, we were able to achieve reasonably good synchronization. Unsynchronized TR9-7 cells show a typical cell cycle distribution with a majority of the cells in G_1 phase and a distinct but small G_2/M phase peak (Figure 1B). After aphidicolin treatment, > 90% of cells were in the G_1 phase (Figure 1B). After incubation with Hoechst 33342, approximately 60% of the cells were in G_2 phase, as characterized using ModFit software to analyze the flow cytometry data (Figure 1B). The approximately 40% of cells remaining in G_1 phase appeared irreversibly arrested in G_1.

p53 expression in cells after G_2 synchronization. p53 levels were assessed in cells during synchronization and after release from G_2 phase. Generally, p53 expression was maintained consistently in cultures with low tetracycline and suppressed by tetracycline at 1,500 ng/mL throughout the experiment (Figure 2). The achievement of a high level of synchrony in the cultures required the moderate expression of p53 that was suppressed by addition of tetracycline at 1,500 ng/mL 6 hr prior to release from G_2 phase blockade. A modest amount of residual p53 was detectable in 1,500 ng/mL tetracylcline cultures [p53$^{(-)}$] at 0 and 3 hr after release, although p53 expression was much lower than that observed in cultures with only 15 ng/mL tetracycline [p53$^{(+)}$].

Arsenite delays mitotic exit selectively in p53$^{(-)}$ cells. We examined arsenite effects on entry into and exit from mitosis in synchronized cells. Mitotic indices and p53

Table 1. Arsenite-dependent gene induction detected by microarray analysis at 0 and 3 hr after release from G_2 phase synchrony with FDR applied.[a]

UniGene ID	Probe set ID	Gene title	Gene symbol	Fold-change p53$^{(+)}$	Fold-change p53$^{(-)}$
517581	33802_at	heme oxygenase (decycling) 1	HMOX1	27.2	26.1
504609	36618_g_at	inhibitor of DNA binding 1	ID1	6.9	4.3
418241	39081_at	metallothionein 2A	MT2A	3.9	3.6
519469	34759_at	solute carrier family 30 (zinc transporter), member 1	SLC30A1	3.2	3.1
504609	36619_r_at	inhibitor of DNA binding 1	ID1	3.8	2.7
504609	36617_at	inhibitor of DNA binding 1	ID1	3.7	2.5
534330	36130_f_at	metallothionein 1E (functional)	MT1E	1.9	1.9
513626	31622_f_at	metallothionein 2A	MT2A	1.9	1.8
284141	33835_at	TSPY-like 4	TSPYL4	1.7	1.9
282326	32168_s_at	Down syndrome critical region gene 1	DSCR1	1.6	1.8
37055	1732_at	fibroblast growth factor 5	FGF5	1.7	1.6
440939	31623_f_at	metallothionein 2A	MT2A	1.6	1.5
105269	33369_at	sterol-C4-methyl oxidase-like	SC4MOL	1.4	1.5
467020	1700_at	BCL2 binding component 3	BBC3	0.7	0.6
503093	32588_s_at	zinc finger protein 36, C3H type-like 2	ZFP36L2	0.4	0.3

[a]Gene annotations from NetAffx (http://www.affymetrix.com/analysis/index.affx).

expression were determined in triplicate cultures exposed or not exposed to 5 μM NaAsO$_2$ and harvested 0, 1, 3, 6, 12, 16, 20 and 24 hr after release from G$_2$ phase synchrony induced by Hoechst 33342 exposure. Mitotic indices were determined only in experiments in which the p53 expression was maintained as expected. The mitotic index of cells not exposed to arsenite peaked 3 hr after release from G$_2$ phase (Figure 3A). There was no difference between p53$^{(+)}$ and p53$^{(-)}$ cells. The mitotic index dropped sharply after 3 hr and was < 1% by 12 hr. The mitotic index started to increase again 24 hr after release from G$_2$ phase, indicating that the cells had started to cycle again. Arsenite treatment delayed the peak in mitotic index to 6 hr after release from G$_2$ phase in both p53$^{(+)}$ and p53$^{(-)}$ cells. The mitotic index of p53$^{(+)}$ cells treated with arsenite decreased after 6 hr and returned to baseline by 16 hr. The slope of the decrease in mitotic index of arsenite-treated p53$^{(+)}$ cells is similar to that of the decline in cells not exposed to arsenite. These results suggest that entry into mitosis is delayed in p53$^{(+)}$ cells but that mitotic exit is normal. In contrast, the mitotic index of p53$^{(-)}$ cells treated with arsenite dropped slowly and was still significantly elevated

16 hr ($p < 0.001$, n = four experiments) after release from G$_2$ phase arrest. The mitotic index dropped to nearly zero by 24 hr after release from G$_2$ phase.

Arsenite induces alteration of expression profiles. Microarray analysis was conducted on mRNAs prepared from p53$^{(+)}$ and p53$^{(-)}$ cells at 0 and 3 hr after release from G$_2$ phase synchrony with or without arsenite exposure. ANOVA of four biological replicates using a $p < 0.05$ was performed with Bioconductor/R software using MAS background correction, quantiles normalization, MAS PM correction, and MAS summary. Analysis was conducted with (Table 1) and without (Tables 2, 3) application of the Benjamini and Hochberg false discovery rate (FDR) correction. Table 1 is all inclusive, whereas Table 2 includes only those genes showing ≥ 2-fold increase in either p53$^{(+)}$ or p53$^{(-)}$ samples. Arsenite induced several genes independently of p53 status. Heme oxygenase 1 (*HMOX1*) showed a dramatic > 25-fold increase in expression. Metallothioneines 2A and 1X and the zinc transporter *SLC30A1* were also induced. Expression of the stress-responsive heat shock protein *HSP70B* was elevated > 7-fold. ID1 was induced 3.7- to 6.9-fold in p53$^{(+)}$ cells and 2.5- to 4.3-fold in p53$^{(-)}$ cells depending

on which of three probe sets was evaluated. Although two-way ANOVA did not indicate that the difference in fold-change between p53$^{(+)}$ and p53$^{(-)}$ cells was statistically significant, Western blot analysis did show ID1 induction that was more extensive and sustained in p53$^{(+)}$ cells (Figure 2). Two-way ANOVA did not identify any genes or which expression was dependent on p53; therefore, Venn analysis was performed with GeneSpring software (Agilent Technologies) on lists of genes altered in p53$^{(+)}$ and p53$^{(-)}$ samples by arsenite treatment. The false discovery rate correction was not applied. This approach identified several genes altered by arsenite in only p53$^{(+)}$ or p53$^{(-)}$ (Table 3). For example, MAP kinase phosphatase 1 (MKP-1) was induced only in p53$^{(+)}$ cells and ubiquitin-conjugating enzyme E2N was induced only in p53$^{(-)}$ cells.

Arsenite induces cytokinesis failure and apoptosis. An example of a mitotic cell undergoing apoptosis in an arsenite-treated culture is shown in Figure 3B. Mitosis, from the start of prophase to the completion of cytokinesis, normally takes < 30 min in these cells. As can be observed in Figure 3B, 30 min elapsed from the time a cell was in late anaphase/early telophase (panel 1) to when the cell collapsed (panel 8). The metaphase plates holding the chromosomes did not change position while the membrane developed multiple blebs (panels 1–4). The chromosomes appeared to partially decondense (panel 5). The cell body collapsed between the plates but the membranes did not fuse to complete cytokinesis (panels 6–8).

Discussion

Arsenite (as either NaAsO$_2$ or As$_2$O$_3$) is known to activate the G$_2$ phase checkpoint (Chen et al. 2002) and to induce mitotic arrest and apoptosis in a variety of cell lines including HeLa (Huang and Lee 1998), U937 (Halicka et al. 2002; McCabe et al. 2000), SV40-transformed human fibroblasts (Halicka et al. 2002; McCabe et al. 2000; States et al. 2002), and several prostate and ovarian carcinoma cells (Uslu et al. 2000). A common feature of the cells in which arsenite induces both mitotic arrest and apoptosis is a functional loss of p53. We have shown that arsenite-induced mitotic arrest occurs in asynchronous cells lacking p53 expression but not in cells expressing p53 (Taylor et al. 2006). In the present study, we have determined whether p53 expression affects the progression of arsenite-treated cells from G$_2$ phase into M phase and/or the exit from mitosis.

TR9-7 cells are a well-characterized model to study p53-dependent processes, taking advantage of tetracycline-regulated p53 expression (Adimoolam and Ford 2002; Agarwal et al. 1995; Ford and Hanawalt 1997; Lloyd and Hanawalt 2002; Robles et al. 2001; Taylor

Table 2. Arsenite-dependent gene induction detected by microarray analysis at 0 and 3 hr after release from G$_2$ phase synchrony with FDR not applied.[a]

UniGene ID	Probe set ID	Gene title	Gene symbol	Fold-change p53$^{(+)}$	p53$^{(-)}$
517581	33802_at	heme oxygenase (decycling) 1	HMOX1	27.2	26.1
3268	35965_at	heat shock 70k protein 6 (HSP70B')	HSPA6	8.5	6.9
504609	36618_g_at	inhibitor of DNA binding 1	ID1	6.9	4.3
520028	1104_s_at	heat shock 70kDa protein 1A	HSPA1A	5.8	4.9
418241	39081_at	metallothionein 2A	MT2A	3.9	3.6
609521	34759_at	solute carrier family 30 (zinc transporter), member 1	SLC30A1	3.2	3.1
504609	36619_r_at	inhibitor of DNA binding 1	ID1	3.8	2.7
504609	36617_at	inhibitor of DNA binding 1	ID1	3.7	2.5
374950	39120_at	metallothionein 1X	MT1X	3.3	4.5
148340	41215_s_at	inhibitor of DNA binding 2	ID2	3.1	2.8
799	38037_at	diphtheria toxin receptor	DTR	2.8	1.9
153863	1955_s_at	SMAD, mothers against DPP homolog 6	SMAD6	2.4	2.0
76884	37043_at	inhibitor of DNA binding 3	ID3	2.4	2.5
491611	1137_at	solute carrier family 20 member 2	SLC20A2	2.2	2.3
517617	36711_at	v-maf musculoaponeurotic fibrosarcoma oncogene	MAFF	2.2	1.9
520819	35303_at	insulin induced gene 1	INSIG1	2.1	1.8
196054	37483_at	histone deacetylase 9	HDAC9	2.1	1.7

[a]Gene annotations from NetAffx (http://www.affymetrix.com/analysis/index.affx).

Table 3. p53-dependent gene induction by arsenite determined by Venn analysis (FDR not applied).[a]

Unigene ID	Probe set ID	Gene title	Gene symbol	Fold-change
P53$^{(+)}$ cells				
520028	31692_at	heat shock 70kDA protein 1A	HSPA1A	4.7
419	34585_at	distal-less homeo box 2	DLX2	2.3
171695	1005_at	dual specificity phosphatase 1 (MKP-1)	DUSP1	2.1
P53$^{(-)}$ cells				
142912	36799_at	frizzled homolog 2 (Drosophila)	FZD2	4.2
50308	40121_at	huntingtin interacting protein 2	HIP2	2.5
93002	1651_at	ubiquitin-conjugating enzyme E2C	UBE2C	2.2
524630	36604_at	ubiquitin-conjugating enzyme E2N	UBE2N	2.2

[a]Gene annotations from NetAffx (http://www.affymetrix.com/analysis/index.affx).

et al. 2001) We synchronized these human fibroblasts in G_2 phase using a multi-step protocol developed by others (Kuhholzer and Prather 2001; Tobey et al. 1990) and adapted to our experiments. The fraction of the cells in G_2 phase was not as high as some investigators have achieved with normal diploid fibroblasts (Tobey et al. 1990) but higher than that achieved by another group (Kuhholzer and Prather 2001).

Our results indicate that arsenite exposure delays progression from G_2 phase to M phase in both p53[(–)] and p53[(+)] cells. This result is consistent with reported arsenite-induced G_2 phase delay (McCollum et al. 2005; Park et al. 2001). However, the exit from mitosis was delayed only in p53[(–)] cells. The mitotic index in arsenite-treated p53[(+)] cells declined with the same kinetics as in untreated cells. The mitotic index declined more slowly in arsenite-treated p53[(–)] cells, suggesting that these cells exit mitosis more slowly. The arsenite-treated cells entered apoptosis while futilely attempting cytokinesis. These data indicate that arsenite delays entry into mitosis and progression to anaphase in TR9-7 cells regardless of p53 expression but that exit from mitosis is p53 dependent in arsenitetreated cells. Thus, both entry into and exit from mitosis is delayed in p53[(–)] cells. Furthermore, the p53[(–)] cells undergo apoptosis as a result of failed or abnormal mitotic exit.

As p53 is a transcription factor, we hypothesized that expression profile changes could contribute to delayed mitotic exit kinetics seen in p53[(–)] cells. To test this, we performed microarray analysis of RNAs prepared from G_2 phase synchronized p53[(+)] and p53[(–)] cells harvested at 0-hr and after 3-hr exposure to 5 μM sodium arsenite. *HMOX1* was highly and rapidly induced, independently of p53. *HMOX1* induction is a well-documented response to arsenite (Andrew et al. 2003; Liu et al. 2001). *HMOX1* induction is associated with cellular response to oxidative damage, as the degradation products of heme are known to scavenge free radicals (Abraham 2003).

The induction of metallothioneins 2A and 3 may also serve a protective role, as metallothionein has been shown to bind arsenicals (Jiang et al. 2003) and metallothionein null mice are hypersensitive to arsenite toxicity (Liu et al. 2000). MKP1, a phosphatase, was induced in p53[(+)] cells and may serve a protective role as it opposes the activation of SAPK/JNK (Li et al. 2003), a kinase involved in the induction of apoptosis by arsenite (Davison et al. 2004), MKP1 is a transcriptional target of p53 (Li et al. 2003) and has been shown to be arsenite-induced (Li et al. 2001). The expression of ID1 was elevated by arsenite and Western blot analysis showed the extent of induction was greater and more sustained in p53[(+)] cells. ID1 is a dominant negative inhibitor of transcription that forms inactive heterodimers with basic helix–loop–helix transcription factors. Genes identified as targets of repression by ID1 include those encoding the cyclin-dependent kinase inhibitory proteins *p15[INK4B]*, *p16[INK4A]*, and *p21[CIP1/WAF1]* (Sikder et al. 2003). Our previous results indicate that the increased sensitivity to mitotic arrest associated apoptosis of p53-deficient cells is due to the lack of p21[CIP1/WAF1], a transcriptional target of p53 (Taylor et al. 2006). p21[CIP1/WAF1] may prevent mitotic arrest associated apoptosis in p53[(+)] cells by allowing for mitotic exit of cells arrested in mitosis. Mitotic exit requires the destruction of cyclin B or inhibition of the cyclin B/CDC2 complex. The promotion of mitotic exit by p21[CIP1/WAF1] would involve its direct inhibition of cyclin B/CDC2 (Taylor and Stark 2001). However, once p53[(+)] cells exit mitosis, cell cycle progression would require the inhibition of p21[CIP1/WAF1]. The induction of ID1 by arsenite may serve to repress p21[CIP1/WAF1] and allow for continued cell cycle progression (Figure 4).

Ectopic overexpression of ID1 immortalizes primary keratinocytes (Alani et al. 1999) and a portion of the ID1 localizes to centrosomes, causing abnormal centrosome number (Hasskarl et al. 2004). Centrosomes serve as the organizational units for the mitotic spindle apparatus. Therefore, an aberrant number of centrosomes may be aneuploidogenic by preventing proper chromosomal segregation. The induction of aneuploidy was posited as the most likely mechanism of arsenic carcinogenesis (NRC 1999, 2001). ID1 also protects against apoptosis through activation of the nuclear factor kappa B signaling pathway (Ling et al. 2003). Higher ID1 levels in p53[(+)] cells may therefore promote survival. ID1 basal levels are elevated in a variety of cancers, and ID1 is induced during malignant transformation of rat liver cells by arsenic (Chen et al. 2001). Consequently, ID1 induction by arsenite may play an important role in the mechanism of arsenic carcinogenesis by allowing for survival of cells progressing through aberrant mitosis and inducing abnormal chromosome numbers.

Loss of p53 function as seen in many tumors has been suggested to allow cells to bypass cell cycle checkpoints after DNA damage and to enter a nonmitotic state (Erenpreisa and Cragg 2001). Our results suggest p53 plays an important role in prevention of arsenite-induced mitotic arrest and also in apoptosis consequent to the arrest. The prevention of mitotic arrest–associated apoptosis is likely a key event in arsenic-induced carcinogenesis because it predisposes cells to aneuploidy. Understanding the link between p53 and prevention of apoptosis associated with arsenite-induced mitotic arrest will provide essential information regarding the mechanism of arsenic carcinogenesis and also help identify a key target for cancer chemotherapeutics.

REFERENCES

Abraham NG. 2003. Therapeutic applications of human heme oxygenase gene transfer and gene therapy. Curr Pharm Des 9:2513–2524.

Adimoolam S, Ford JM. 2002. p53 and DNA damage-inducible expression of the xeroderma pigmentosum group C gene. Proc Natl Acad Sci USA 99:12985–12990.

Agarwal ML, Agarwal A, Taylor WR, Stark GR. 1995. p53 controls both the G_2/M and the G_1 cell cycle checkpoints and mediates reversible growth arrest in human fibroblasts. Proc Natl Acad Sci USA 92:8493–8497.

Alani RM, Hasskarl J, Grace M, Hernandez MC, Israel MA, Munger K. 1999. Immortalization of primary human keratinocytes by the helix-loop-helix protein, Id-1. Proc Natl Acad Sci USA 96:9637–9641.

Andrew AS, Warren AJ, Barchowsky A, Temple KA, Klei L, Soucy NV, et al. 2003. Genomic and proteomic profiling of responses to toxic metals in human lung cells. Environ Health Perspect 111:825–835.

Chen F, Zhang Z, Bower J, Lu Y, Leonard SS, Ding M, et al. 2002. Arsenite-induced Cdc25C degradation is through the KEN-box and ubiquitin-proteasome pathway. Proc Natl Acad Sci USA 99:1990–1995.

Chen H, Liu J, Merrick BA, Waalkes MP. 2001. Genetic events associated with arsenic-induced malignant transformation: applications of cDNA microarray technology. Mol Carcino 30:79–87.

Cohen MH, Hirschfeld S, Flamm HS, Ibrahim A, Johnson JR, O'Leary JJ, et al. 2001. Drug approval summaries: arsenic trioxide, tamoxifen citrate, anastrazole, paclitaxel, bexarotene. Oncologist 6:4–11.

Davison K, Mann KK, Waxman S, Miller WH, Jr. 2004. JNK activation is a mediator of arsenic trioxide-induced apoptosis in acute promyelocytic leukemia cells. Blood 103:3496–3502.

Du YH, Ho PC. 2001. Arsenic compounds induce cytotoxicity and apoptosis in cisplatin-sensitive and -resistant gynecological cancer cell lines. Cancer Chemother Pharmacol 47:481–490.

Erenpreisa J, Cragg MS. 2001. Mitotic death: a mechanism of survival? A review. Cancer Cell Int 1:1. Available: http://www.cancerci.com/content/1/1/1 [accessed 9 August 2006].

Ford JM, Hanawalt PC. 1997. Expression of wild-type p53 is required for efficient global genomic nucleotide excision repair in UV-irradiated human fibroblasts. J Biol Chem 272:28073–28080.

Halicka HD, Smolewski P, Darzynkiewcz Z, Dai W, Traganos F. 2002. Arsenic trioxide arrests cells early in mitosis leading to apoptosis. Cell Cycle 1:201–209.

Hasskarl J, Duensing S, Manuel E, Munger K. 2004. The helix-loop-helix protein ID1 localizes to centrosomes and rapidly induces abnormal centrosome numbers. Oncogene 23:1930–1938.

Huang SC, Lee TC. 1998. Arsenite inhibits mitotic division and perturbs spindle dynamics in HeLa S3 cells. Carcinogenesis 19:889–896.

Jiang G, Gong Z, Li XF, Cullen WR, Le XC. 2003. Interaction of trivalent arsenicals with metallothionein. Chem Res Toxicol 16:873–880.

Jin S, Levine AJ. 2001. The p53 functional circuit. J Cell Sci 114:4139–4140.

Kuhholzer B, Prather RS. 2001. Synchronization of porcine fetal fibroblast cells with topoisomerase-inhibitor Hoechst 33342. Anim Reprod Sci 66:109–116.
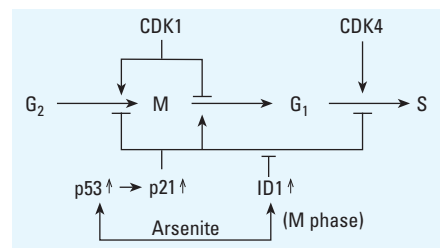
Figure 4. Model for exit from mitotic arrest induced by arsenite and subsequent cell cycle progression dependent on p21[CIP1/WAF1] and ID1 induction in p53-expressing cells.

Li J, Gorospe M, Hutter D, Barnes J, Keyse SM, Liu Y. 2001. Transcriptional induction of MKP-1 in response to stress is associated with histone H3 phosphorylation-acetylation. Mol Cell Biol 21:8213–8224.

Li M, Zhou JY, Ge Y, Matherly LH, Wu GS. 2003. The phosphatase MKP1 is a transcriptional target of p53 involved in cell cycle regulation. J Biol Chem 278:41059–41068.

Ling MT, Wang X, Ouyang XS, Xu K, Tsao SW, Wong YC. 2003. Id-1 expression promotes cell survival through activation of NF-kappaB signalling pathway in prostate cancer cells. Oncogene 22:4498–4508.

Liu J, Kadiiska MB, Liu Y, Lu T, Qu W, Waalkes MP. 2001. Stress-related gene expression in mice treated with inorganic arsenicals. Toxicol Sci 61:314–320.

Liu J, Liu Y, Goyer RA, Achanzar W, Waalkes MP. 2000. Metallothionein-I/II null mice are more sensitive than wild-type mice to the hepatotoxic and nephrotoxic effects of chronic oral or injected inorganic arsenicals. Toxicol Sci 55:460–467.

Lloyd DR, Hanawalt PC. 2002. p53 controls global nucleotide excision repair of low levels of structurally diverse benzo(g)chrysene-DNA adducts in human fibroblasts. Cancer Res 62:5288–5294.

Maeda H, Hori S, Nishitoh H, Ichijo H, Ogawa O, Kakehi Y, et al. 2001. Tumor growth inhibition by arsenic trioxide (As_2O_3) in the orthotopic metastasis model of androgen-independent prostate cancer. Cancer Res 61:5432–5440.

McCabe MJ Jr, Singh KP, Reddy SA, Chelladurai B, Pounds JG, Reiners JJ Jr, et al. 2000. Sensitivity of myelomonocytic leukemia cells to arsenite-induced cell cycle disruption, apoptosis, and enhanced differentiation is dependent on the inter-relationship between arsenic concentration, duration of treatment, and cell cycle phase. J Pharmacol Exp Ther 295:724–733.

McCollum G, Keng PC, States JC, McCabe MJ. 2005. Arsenite delays progression through each cell cycle phase and induces apoptosis following G_2/M arrest in U937 myeloid leukemia cells. J Pharmacol Exp Ther 313:877–887.

NRC (National Research Council). 1999. Arsenic in Drinking Water. Washington DC:National Academy Press.

NRC (National Research Council). 2001. Arsenic in Drinking Water:2001 Update. Washington DC:National Academy Press.

Park JW, Choi YJ, Jang MA, Baek SH, Lim JH, Passaniti T, et al. 2001. Arsenic trioxide induces G_2/M growth arrest and apoptosis after caspase-3 activation and bcl-2 phosphorylation in promonocytic U937 cells. Biochem Biophys Res Commun 286:726–734.

Robles AI, Bemmels NA, Foraker AB, Harris CC. 2001. APAF-1 is a transcriptional target of p53 in DNA damage-induced apoptosis. Cancer Res 61:6660–6664.

Sikder HA, Devlin MK, Dunlap S, Ryu B, Alani RM. 2003. Id proteins in cell growth and tumorigenesis. Cancer Cell 3:525–530.

States JC, Reiners JJ Jr, Pounds JG, Kaplan DJ, Beauerle BD, McNeely SC, et al. 2002. Arsenite disrupts mitosis and induces apoptosis in SV40-transformed human skin fibroblasts. Toxicol Appl Pharmacol 180:83–91.

Taylor BF, McNeely SC, Miller HL, Lehmann GM, McCabe MJ Jr, States JC. 2006. p53 suppression of arsenite-induced mitotic catastrophe is mediated by p21[CIP1/WAF1]. J Pharmacol Exp Ther 318:142–151.

Taylor WR, Schonthal AH, Galante J, Stark GR. 2001. p130/E2F4 binds to and represses the cdc2 promoter in response to p53. J Biol Chem 276:1998–2006.

Taylor WR, Stark GR. 2001. Regulation of the G_2/M transition by p53. Oncogene 20:1803–1815.

Tobey RA, Oishi N, Crissman HA. 1990. Cell cycle synchronization: reversible induction of G_2 synchrony in cultured rodent and human diploid fibroblasts. Proc Natl Acad Sci USA 87:5104–5108.

Uslu R, Sanli UA, Sezgin C, Karabulut B, Terzioglu E, Omay SB, et al. 2000. Arsenic trioxide-mediated cytotoxicity and apoptosis in prostate and ovarian carcinoma cell lines. Clin Cancer Res 6:4957–4964.

Vega L, Gonsebatt ME, Ostrosky-Wegman P. 1995. Aneugenic effect of sodium arsenite on human lymphocytes in vitro: an individual susceptibility effect detected. Mutat Res 334:365–373.

Yih LH, Ho IC, Lee TC. 1997. Sodium arsenite disturbs mitosis and induces chromosome loss in human fibroblasts. Cancer Res 57:5051–5059.

Yih LH, Lee TC. 2000. Arsenite induces p53 accumulation through an ATM-dependent pathway in human fibroblasts. Cancer Res 60:6346–6352.

Yin Y, Tainsky MA, Bischoff FZ, Strong LC, Wahl GM. 1992. Wild-type p53 restores cell cycle control and inhibits gene amplification in cells with mutant p53 alleles. Cell 70:937–948.